

Prediction of the Reactivity of Argon with Xenon under High Pressure

Xiao Z. Yan,^{1,2} Yang M. Chen,^{1,2} and Hua Y. Geng,^{1,*}

¹*National Key Laboratory of Shock Wave and Detonation Physics, Institute of Fluid Physics,*

CAEP; P.O. Box 919-102, Mianyang, Sichuan, People's Republic of China, 621900

²*School of Science, Jiangxi University of Science and Technology, Ganzhou, Jiangxi, People's*

Republic of China, 341000

ABSTRACT

Pressure significantly modifies the microscopic interactions in condensed phase, leading to new patterns of bonding and unconventional chemistry. Both argon and xenon possess closed-shell electronic structures, which renders them chemically unreactive. Using unbiased structure searching techniques combined with first-principles calculations, we demonstrate the reaction of argon with xenon at a pressure as low as 1.1 GPa, producing a novel van der Waals compound XeAr_2 , which crystallizes in the MgCu_2 -type Laves phase structure. Due to the pressure-induced delocalization of the electrons in outermost shells, the covalent Xe-Xe and Xe-Ar bonds have been detected which lead XeAr_2 to be unexpectedly stable without any phase transition or decomposition at least up to 500 GPa.

*To whom correspondence should be addressed. Email: s102genghy@caep.cn.

1. INTRODUCTION

Due to the stable closed-shell electronic configuration, noble gas (NG) elements (e.g. He, Ne, Ar, Kr and Xe) were historically believed to be chemically unreactive. However, Pauling¹ predicted that Xe and Kr may bond to electronegative atoms, which was proved experimentally by Bartlett² with the synthesis of first NG compound XePtF₆. This seminal discovery led to a recognized renaissance in NG chemistry in the past few decades³⁻⁵.

Under ambient conditions, the heavier NG element Xe, and to some extent, Kr and Ar, have been known to be oxidized by halogen and oxygen, forming halide and oxide compounds⁶⁻⁸. Under high pressures, the reactivity of NGs was drastically altered.

On one hand, application of high pressure makes NGs easier to be oxidized; for example, NGs can be oxidized not only by fluorine⁹⁻¹² and oxygen¹³⁻¹⁶, but also nitrogen¹⁷ and sulphur¹⁸, and even metal elements such as iron and nickel¹⁹. Theoretical predictions revealed that Xe reacts with S and N at 146 GPa¹⁷ and 191 GPa¹⁸, respectively. Direct reactions of Xe with Fe/Ni were predicted to occur under the pressures of Earth's inner core¹⁹. A subsequent experimental study reported the synthesis of Xe-Ni compound at a pressure round 150 GPa²⁰. Of special attention, the Fe/Ni atoms in the Xe-Fe/Ni compounds play a role of anions instead of cations that behave as usual metals. In addition, Xe has also been observed to react with water ice at pressures above 50 GPa²¹. In these NG compounds, Xe bonds to other elements chemically by sharing its closed shell electrons. On the contrary, NG elements can also become oxidants and gain electrons from alkali and alkaline earth metals such as Li²², Cs²³ and Mg²⁴.

On the other hand, NGs also form van der Waals (vdW) compounds under lower pressures wherein the NG atoms do not lose or gain electrons. For instance, the Laves phases compounds NeHe₂²⁵, ArHe₂²⁶, Ar(H₂)₂²⁷, Xe(N₂)₂^{28,29} and Xe(O₂)₂³⁰ can be synthesized at pressures of a few gigapascals. The stabilities of such compounds can be explained in terms of packing rules analogous to binary crystals of hard spherelike particles for intermetallic compounds. Other classes of vdW compounds have also been discovered. (N₂)₆Ne₇³¹, the structure can be viewed as a clathrate with the centers of the N₂ molecules forming distorted dodecahedron cages, each enclosing 14 Ne atoms. XeHe₂³² stabilizes at 12 GPa, adopting a hexagonal AlB₂-type structure. Some other stoichiometries such as the Xe-H₂³³⁻³⁵, Xe-H₂O³⁶ and He-H₂O^{37 38} systems have also been observed. The origin of the stability for these compounds was not well understood.

In a few cases, unexpected chemistry in Xe-F compounds stabilized by covalent Xe-Xe bonding⁹ and in Na₂He compound stabilized by long-range Coulomb interactions³⁹ have also been reported. It is obvious that the bonding of NGs in compounds under high pressures exhibits strong uncertainty, which provides a very broad scenario waiting for further investigation.

In this paper, we theoretically explore the phase diagram and bonding of Xe-Ar binary system under high pressures. Our results demonstrate the existence of a Xe-Ar compound with the stoichiometry of XeAr₂. Due to the fact that both of Ar and Xe have filled valence shells, this compound is bound by vdW forces under low pressures. However, high pressures modified substantially the atomic interactions in this compound and strong covalent bonds have been detected.

2. COMPUTATIONAL DETAILS

We perform a systematic structural search for the Xe-Ar binary system based on a particle swarm optimization methodology as implemented in the CALYPSO code^{40,41}, which has been successfully employed in predicting a large variety of crystal structures^{9,17-19,42-44}. The underlying total energy calculations and structural relaxations are carried out within the framework of density functional theory using the projector-augmented-wave (PAW) method⁴⁵ as implemented in the VASP code⁴⁶. We adopt the Perdew-Burke-Ernzerh of generalized gradient approximation⁴⁷ to describe the exchange–correlation functional. The electron-ion interaction is described by pseudopotentials with 5s²5p⁶ and 3s²3p⁶ as valence electrons for Xe and Ar, respectively. The use of a cutoff energy of 650 eV and dense enough k-point sampling grids give excellent convergence of the calculated enthalpy (<1 meV/atom). The dynamical stability of predicted structures is determined by phonon calculations using the finite displacement approach as implemented in the Phonopy code⁴⁸.

3. RESULTS AND DISCUSSION

In order to obtain the most energetically favorable structures for the Xe-Ar binary system, the stoichiometries of XeAr_{*n*} (*n* = 1-8) containing up to 4 formula units (f.u.) per simulation cell are systematically searched under pressures of 0, 100, 200 and 500 GPa. The calculated formation enthalpies (*H^f*) of each stoichiometry at different pressures are shown in the form of convex hulls as depicted in Figure 1. From this figure, the thermodynamic stability of XeAr_{*n*} can be determined. The results indicate that each stoichiometry of XeAr_{*n*} has a small positive *H^f* at 0 GPa. As pressure

increase to 100, 200 or 500 GPa, the convex hulls are dominated by a well-developed minimum at XeAr_2 stoichiometry, indicating that only XeAr_2 is stable against decomposition into elemental Xe and Ar. The other stoichiometries are thermodynamically unstable due to the fact that the increase of pressure would promote their formation enthalpies to be more positive.

The stable XeAr_2 compound is predicted to crystallize in the MgCu_2 -type Lave phase structure (Figure 2a), wherein the Xe atoms occupy the Mg (8a) sites, forming a diamond-type sublattice, and the Ar atoms reside in the voids of the Xe framework, occupying the Cu (16d) sites. By representing its constituents as hard spheres, the stability of AB_2 -type Lave phase can be understood by packing rule, i.e., a hard-sphere radius ratio R_A/R_B close to 1.25 will achieve the maximum packing efficiency (0.71%) when crystallize in Lave phase⁴⁹. The ratio R_A/R_B of XeAr_2 is 1.13, which is close to the ideal value of a Laves phase. Our structural search simulations reveal that the increase of pressure will further stabilize the Laves phase XeAr_2 , instead of any phase transition or decomposition, which is in sharp distinction with other NG compounds such as XeHe_2 ³², NeHe_2 ²⁶ and ArHe_2 ²⁶.

The inset of Figure 1 shows the pressure-dependent formation enthalpy of MgCu_2 -type XeAr_2 wherein it is shown that XeAr_2 becomes stable at 1.1 GPa. The effect of vdW interactions on the stability of XeAr_2 is also calculated by using the PBE-D2 method⁵⁰. The results indicate that the stable pressure shifts to 2.6 GPa with the inclusion of vdW corrections. To determine the dynamical stability of MgCu_2 -type XeAr_2 , the phonon dispersion spectra are calculated based on the quasi-harmonic model, and the selected results are shown in Figure 3. It is found that XeAr_2 is dynamically stable without showing any imaginary phonon frequency in the pressure range from 5 GPa to 500 GPa.

It is known that the Gibbs free energy ($G = H - TS$) reduces to enthalpy ($H = U + pV$) when temperature is 0 K. The formation enthalpy of a compound is determined by the relative internal energy ΔU and $p\Delta V$ term with respect to elemental solids. The calculated pressure dependence of ΔU and $p\Delta V$ of XeAr_2 are shown in Figure 4. It is obvious that the $p\Delta V$ term has negative values over the pressure range considered. The large gain in $p\Delta V$ term effectively tunes the formation enthalpy to be negative though the relative internal energies ΔU are positive at 0–150 GPa, leading to the reaction of Xe with Ar above 1.1 GPa. The negative $p\Delta V$ of XeAr_2 is attributed to the smaller volume compared to the mixing volume of elemental Xe and Ar. For comparison, we

also calculated the pressure dependent $p\Delta V$ for MgCu₂-type XeS₂¹⁸ and AlB₂-type XeHe₂³². As shown in Figure 4, the $p \sim p\Delta V$ curve of XeS₂ is similar to that of XeAr₂, being negative in the whole pressure region considered. While the results of XeHe₂ is negative under low pressures but becomes to be positive under high pressures. In other words, the pressure induced close-packed MgCu₂-type XeS₂ and XeAr₂ make themselves energetically more favorable than the elemental solids in the whole pressure region considered, whereas the AlB₂-type XeHe₂ which adopts a layered structure would stabilize at low pressures but decompose at high pressures³².

To get further insight into the stabilized mechanism, we calculated the electronic properties and atomic interactions of XeAr₂ under high pressures.

Figure 5 shows the calculated projected density of states (PDOS) at different pressures. It is clear that XeAr₂ is a wide-gap insulator under low pressures. At 10 GPa, the band gap is 8.0 eV (Figure 5a). The Ar 3s and Xe 5s electrons occupy the lowest states of valence band located at -17.5 eV and -12.5 eV, respectively. The states range from -5.5 eV to 0 eV are predominantly composed of Ar 3p and Xe 5p components mixed with a small contribution from Ar 3p and Xe 5p. All of these states are highly localized, which suggest a weak interaction between Xe and Ar. As pressure increases, the band gap decreases slowly, and the metallization occurs at about 500 GPa (Figure 2b). Under high pressure, as can be seen from the PDOS plotted in Figure 5b, the electronic states are wildly broadened, indicating the relevant valence electrons become more delocalized. Moreover, the PDOS shows a significant overlap between the 5p states of Xe and the 3p states of Ar. Visible overlaps also exist between other states, such as the Ar 3s and Xe 5p, and the Xe 5s and Ar 3p states. Additionally, Bader analysis⁵¹ reveals a charge transfer of 0.43 *e*/atom from Xe to Ar at 500 GPa (Figure 2C). These features of electronic properties indicate strong chemical interactions in the XeAr₂ compound.

Given the fact that NG atoms have filled valence shells, two NG atoms always do not engage in chemical bonding. However, the pressure induced formation of Xe–Xe covalent bond is predicted in a Xe₂F compound, which is the first example of NG-NG bond. For XeAr₂ that composed by two NG elements, the nearest Xe-Xe, Xe-Ar and Ar-Ar distances at 500 GPa are 2.56 Å, 2.45 Å and 2.09 Å, respectively. These atomic distances are close enough for them to form covalent bonds compared with the proposed covalent radius of Xe (1.40 Å) and Ar (1.06 Å) atoms⁵². To detect the covalent bonding in XeAr₂, we calculate the Crystalline Orbital

Hamiltonian Population (COHP) for nearest-neighboring Xe-Xe, Xe-Ar and Ar-Ar pairs. As can be seen from Figure 5c, the contributions from bonding states are larger than that from antibonding in the occupied states of Xe-Xe pair. As a result, the integrated COHP (ICOHP) up to the Fermi level is -1.20 eV/pair for bonded Xe-Xe, indicating a strong covalent bonding. Furthermore, we also calculate the electron localization function (ELF)⁵³ of XeAr₂ at 500 GPa (Figure 2d). The observed large ELF basins (~0.5) confirm the presence of covalent Xe-Xe bonds. The COHP plots of Xe-Ar and Ar-Ar pairs show that the visible overlaps of the Ar 3s, Ar 3p, Xe 5s and Xe 5p states range from -35 to -15 eV are also related to the covalent bonding. However, because of the large occupation of the antibonding states, the ICOHP of Xe-Ar is -0.36, indicating a weaker covalent bonding. The obtained smaller ELF values (0.32) between the neighboring Xe-Ar atoms and the ELF distributions of Ar atoms depart from sphericity also confirm this. The bonding of neighboring Ar-Ar atoms is much weaker since the ICOHP is only -0.07.

4. CONCLUSIONS

In summary, we have theoretically explored the stability of XeAr_n ($n = 1-8$) under high pressures up to 500 GPa using the effective CALYPSO structure searching method combined with first-principles calculations. The results shown that Xe reacts with Ar at a pressure as low as 1.1 GPa, producing a MgCu₂-type Lave phase XeAr₂ compound. This compound is a wide-gap insulator which would metallizes at about 500 GPa. Analysis of the electronic structures and atomic interactions indicates the vdW XeAr₂ compound under low pressures would change to an extended solid wherein atoms are bonded by network of covalent bonds under high pressures. Our results shed light on the chemical bonding between NG elements and enrich NG chemistry.

ACKNOWLEDGMENTS

This work is supported by the National Natural Science Foundation of China under Grant Nos. 11672274 and 11274281, the CAEP Research Projects under Grant Nos. 2012A0101001 and 2015B0101005, the NSAF under Grant No. U1730248, and the Fund of National Key Laboratory of Shock Wave and Detonation Physics of China under Grant No. 6142A03010101.

References

- (1) Pauling, L. The formulas of antimononic acid and the antimonates. *J. Am. Chem. Soc.* **1933**, *55*, 1895.
- (2) Bartlett, N. Xenon hexafluoroplatinate(V) $\text{Xe}^+[\text{PtF}_6]^-$. *Proc. Chem. Soc.* **1962**, *6*, 197.
- (3) Grochala, W. Atypical compounds of gases, which have been called ‘noble’. *Chem. Soc. Rev.* **2007**, *36*, 1632.
- (4) Gerber, R. B. Formation of novel rare-gas molecules in low-temperature matrices. *Annu. Rev. Phys. Chem.* **2004**, *55*, 55.
- (5) Haner, J.; Schrobilgen, G. J. The Chemistry of Xenon(IV). *Chem. Rev.* **2015**, *115*, 1255.
- (6) Levy, H. A.; Agron, P. A. The crystal and molecular structure of xenon difluoride by neutron diffraction. *J. Am. Chem. Soc.* **1963**, *85*, 241.
- (7) Templeton, D. H.; Zalkin, A.; Forrester, J.; Williamson, S. M. Crystal and molecular structure of xenon trioxide. *J. Am. Chem. Soc.* **1963**, *85*, 817.
- (8) Khriachtchev, L.; Pettersson, M.; Runeberg, N.; Lundell, J.; Räsänen, M. A stable argon compound. *Nature* **2000**, *406*, 874.
- (9) Peng, F.; Botana, J.; Wang, Y.; Ma, Y.; Miao, M. Unexpected Trend in Stability of Xe-F Compounds under Pressure Driven by Xe-Xe Covalent Bonds. *J. Phys. Chem. Lett.* **2016**, *7*, 4562.
- (10) Kim, M.; Debessai, M.; Yoo, C.-S. Two- and three-dimensional extended solids and metallization of compressed XeF_2 . *Nature Chem.* **2010**, *2*, 784.
- (11) Dominik, K. O.; Patryk, Z. E.; Wojciech, G.; Roald, H. Freezing in resonance structures for better packing: XeF_2 becomes $(\text{XeF}^+)(\text{F}^-)$ at large compression. *Inorg. Chem.* **2011**, *50*, 3832.
- (12) Braïda, B.; Hiberty, P. C. The essential role of charge-shift bonding in hypervalent prototype XeF_2 . *Nature Chem.* **2013**, *5*, 417.
- (13) Zhu, Q.; Jung, D. Y.; Oganov, A. R.; Glass, C. W.; Gatti, C.; Lyakhov, A. O. Stability of xenon oxides at high pressures. *Nature Chem.* **2013**, *5*, 61.
- (14) Dewaele, A.; Worth, N.; Pickard, C. J.; Needs, R. J.; Pascarelli, S.; Mathon, O.; Mezouar, M.; Irifune, T. Synthesis and stability of xenon oxides Xe_2O_5 and Xe_3O_2 under pressure. *Nature Chem.* **2016**, *8*, 784.
- (15) Brock, D. S.; Schrobilgen, G. J. Synthesis of the missing oxide of xenon, XeO_2 , and its implications for Earth's missing xenon. *J. Am. Chem. Soc.* **2011**, *133*, 6265.
- (16) Hermann, A.; Schwerdtfeger, P. Xenon Suboxides Stable under Pressure. *J. Phys. Chem. Lett.* **2014**, *5*, 4336.
- (17) Peng, F.; Wang, Y.; Wang, H.; Zhang, Y.; Ma, Y. Stable xenon nitride at high pressures. *Phys. Rev. B* **2015**, *92*, 094104.
- (18) Yan, X.; Chen, Y.; Xiang, S.; Kuang, X.; Bi, Y.; Chen, H. High-temperature- and high-pressure-induced formation of the Laves-phase compound XeS_2 . *Phys. Rev. B* **2016**, *93*, 214112.
- (19) Zhu, L.; Liu, H.; Pickard, C. J.; Zou, G.; Ma, Y. Reactions of xenon with iron and nickel are predicted in the Earth's inner core. *Nature Chem.* **2014**, *6*, 644.
- (20) Dewaele, A.; Pépin, C. M.; Geneste, G.; Garbarino, G. Reaction between nickel or iron and xenon under high pressure. *High Pressure Res.* **2016**, *37*, 137.
- (21) Sanloup, C.; Bonev, S. A.; Hochlaf, M.; Maynard-Casely, H. E. Reactivity of xenon with ice at planetary conditions. *Phys. Rev. Lett.* **2013**, *110*, 265501.
- (22) Li, X.; Hermann, A.; Peng, F.; Lv, J.; Wang, Y.; Wang, H.; Ma, Y. Stable Lithium Argon compounds under high pressure. *Sci. Rep.* **2015**, *5*, 16675.

- (23) Zhang, S.; Bi, H.; Wei, S.; Wang, J.; Li, Q.; Ma, Y. Crystal Structures and Electronic Properties of Cesium Xenides at High Pressures. *J. Phys. Chem. C* **2015**, *119*, 24996.
- (24) Miao, M.-s.; Wang, X.-l.; Brgoch, J.; Spera, F.; Jackson, M. G.; Kresse, G.; Lin, H.-q. Anionic Chemistry of Noble Gases: Formation of Mg–NG (NG = Xe, Kr, Ar) Compounds under Pressure. *J. Am. Chem. Soc.* **2015**, *137*, 14122.
- (25) Loubeyre, P.; Jean-Louis, M.; LeToullec, R.; Charon-Gérard, L. High pressure measurements of the He–Ne binary phase diagram at 296 K: Evidence for the stability of a stoichiometric Ne(He)₂ solid. *Phys. Rev. Lett.* **1993**, *70*, 178.
- (26) Cazorla, C.; Errandonea, D.; Sola, E. High-pressure phases, vibrational properties, and electronic structure of Ne (He)₂ and Ar (He)₂: A first-principles study. *Phys. Rev. B* **2009**, *80*, 064105.
- (27) Loubeyre, P.; Letoullec, R.; Pinceaux, J.-P. Compression of Ar(H₂)₂ up to 175 GPa: A new path for the dissociation of molecular hydrogen? *Phys. Rev. Lett.* **1994**, *72*, 1360.
- (28) Laniel, D.; Weck, G.; Loubeyre, P. Xe(N₂)₂ compound to 150 GPa: Reluctance to the formation of a xenon nitride. *Phys. Rev. B* **2016**, *94*, 174109.
- (29) Howie, R. T.; Turnbull, R.; Binns, J.; Frost, M.; Dalladay-Simpson, P.; Gregoryanz, E. Formation of xenon-nitrogen compounds at high pressure. *Sci. Rep.* **2016**, *6*, 34896.
- (30) Weck, G.; Dewaele, A.; Loubeyre, P. Oxygen/noble gas binary phase diagrams at 296 K and high pressures. *Phys. Rev. B* **2010**, *82*, 014112.
- (31) Plisson, T.; Weck, G.; Loubeyre, P. (N₂)₆Ne₇: A High Pressure van der Waals Insertion Compound: A High Pressure van der Waals Insertion Compound. *Phys. Rev. Lett.* **2014**, *113*, 025702.
- (32) Wang, Y.; Zhang, J.; Liu, H.; Yang, G. Prediction of the Xe–He binary phase diagram at high pressures. *Chem. Phys. Lett.* **2015**, *640*, 115.
- (33) Somayazulu, M.; Dera, P.; Goncharov, A. F.; Gramsch, S. A.; Liermann, P.; Yang, W.; Liu, Z.; Mao, H.-k.; Hemley, R. J. Pressure-induced bonding and compound formation in xenon–hydrogen solids. *Nature Chem.* **2009**, *2*, 50.
- (34) Somayazulu, M.; Dera, P.; Smith, J.; Hemley, R. J. Structure and stability of solid Xe (H₂)_n. *J. Chem. Phys.* **2015**, *142*, 104503.
- (35) Yan, X.; Chen, Y.; Kuang, X.; Xiang, S. Structure, stability, and superconductivity of new Xe–H compounds under high pressure. *J. Chem. Phys.* **2015**, *143*, 124310.
- (36) Sanloup, C.; Mao Hk, H. K.; Hemley, R. J. High-pressure transformations in xenon hydrates. *Proc. Natl. Acad. Sci. USA* **2002**, *99*, 25.
- (37) Liu, H.; Yao, Y.; Klug, D. D. Stable structures of He and H₂O at high pressure. *Phys. Rev. B* **2015**, *91*, 014102.
- (38) Kuhs, W. F.; Hansen, T. C.; Falenty, A. Filling Ices with Helium and the Formation of Helium Clathrate Hydrate. *J. Phys. Chem. Lett.* **2018**, *9*, 3194.
- (39) Dong, X.; Oganov, A. R.; Goncharov, A. F.; Stavrou, E.; Lobanov, S.; Saleh, G.; Qian, G.-R.; Zhu, Q.; Gatti, C.; Deringer, V. L.; Dronskowski, R.; Zhou, X.-F.; Prakapenka, V. B.; Konôpková, Z.; Popov, I. A.; Boldyrev, A. I.; Wang, H.-T. A stable compound of helium and sodium at high pressure. *Nature Chem.* **2017**, *9*, 440.
- (40) Wang, Y.; Lv, J.; Zhu, L.; Ma, Y. CALYPSO: A method for crystal structure prediction. *Comput. Phys. Commun.* **2012**, *183*, 2063.
- (41) Wang, Y.; Lv, J.; Zhu, L.; Ma, Y. Crystal structure prediction via particle-swarm optimization. *Phys. Rev. B* **2010**, *82*, 094116.
- (42) Chen, Y.; Geng, H. Y.; Yan, X.; Sun, Y.; Wu, Q.; Chen, X. Prediction of Stable Ground-State

- Lithium Polyhydrides under High Pressures. *Inorg. Chem.* **2017**, *56*, 3867.
- (43) Zhong, X.; Yang, L.; Qu, X.; Wang, Y.; Yang, J.; Ma, Y. Crystal Structures and Electronic Properties of Oxygen-rich Titanium Oxides at High Pressure. *Inorg. Chem.* **2018**, *57*, 3254.
- (44) Li, Q.; Zhang, X.; Liu, H.; Wang, H.; Zhang, M.; Li, Q.; Ma, Y. Structural and mechanical properties of platinum carbide. *Inorg. Chem.* **2014**, *53*, 5797.
- (45) Blöchl, P. E. Projector augmented-wave method. *Phys. Rev. B* **1994**, *50*, 17953.
- (46) Kresse, G.; Furthmüller, J. Efficient iterative schemes for ab initio total-energy calculations using a plane-wave basis set. *Phys. Rev. B* **1996**, *54*, 11169.
- (47) Perdew, J. P.; Burke, K.; Ernzerhof, M. Generalized gradient approximation made simple. *Phys. Rev. Lett.* **1996**, *77*, 3865.
- (48) Togo, A.; Oba, F.; Tanaka, I. First-principles calculations of the ferroelastic transition between rutile-type and CaCl₂-type SiO₂ at high pressures. *Phys. Rev. B* **2008**, *78*, 134106.
- (49) Stein, F.; Palm, M.; Sauthoff, G. Structure and stability of Laves phases. Part I. Critical assessment of factors controlling Laves phase stability. *Intermetallics*. **2004**, *12*, 713.
- (50) Grimme, S. Semiempirical GGA-type density functional constructed with a long-range dispersion correction. *J. Comput. Chem.* **2006**, *27*, 1787.
- (51) Bader, R. F. *Atoms in molecules*; Wiley Online Library, 1990.
- (52) Cordero, B.; Gómez, V.; Platero-Prats, A. E.; Revés, M.; Echeverría, J.; Cremades, E.; Barragán, F.; Alvarez, S. Covalent radii revisited. *Dalton Trans.* **2008**, 2832.
- (53) Becke, A. D.; Edgecombe, K. E. A simple measure of electron localization in atomic and molecular systems. *J. Chem. Phys.* **1990**, *92*, 5397.

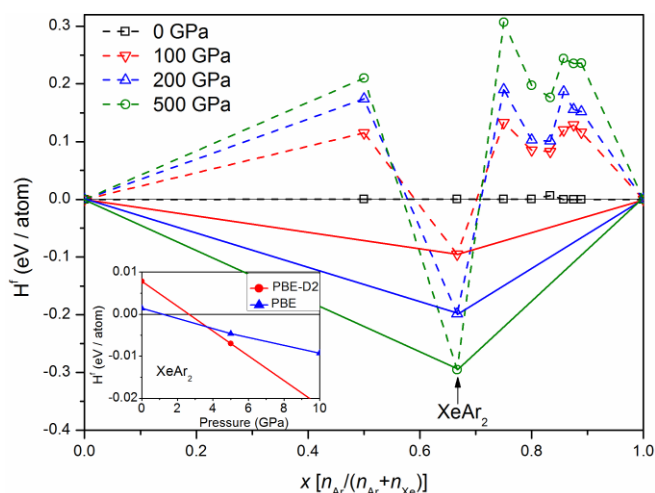


Figure 1. Formation enthalpies (H^f) of XeAr_n ($n = 1-8$) with respect to decomposition into constituent elemental solids under different pressures. Solid lines denote the convex hull, where the data points located on represent stable species against any type of decomposition. Inset: Pressure-dependent formation enthalpy of XeAr_2 obtained with (PBE + D2) and without (PBE) vdW corrections.

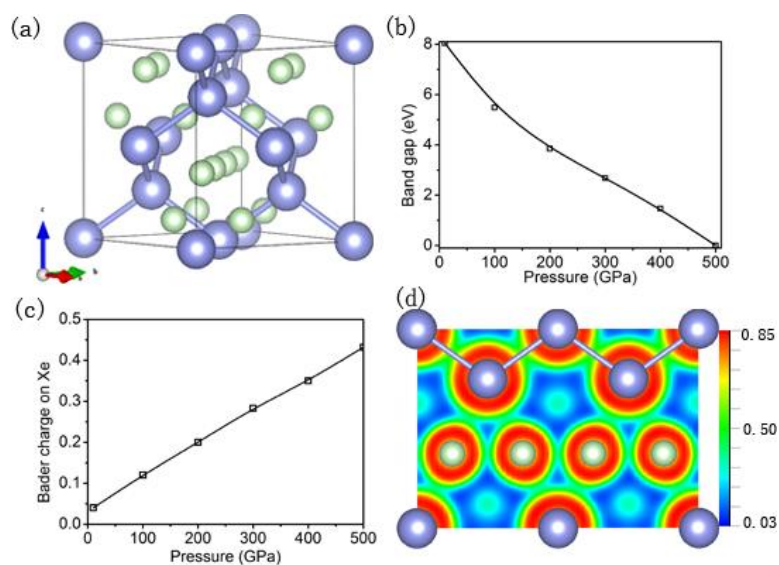


Figure 2. (a) Crystal structure of XeAr_2 . The big and small spheres represent Xe and Ar, respectively. (b) Pressure-dependent band gap of XeAr_2 . (c) Pressure-dependent Bader charge on the Xe atoms in XeAr_2 . (d) Electron localization function (ELF) of XeAr_2 at 500 GPa.

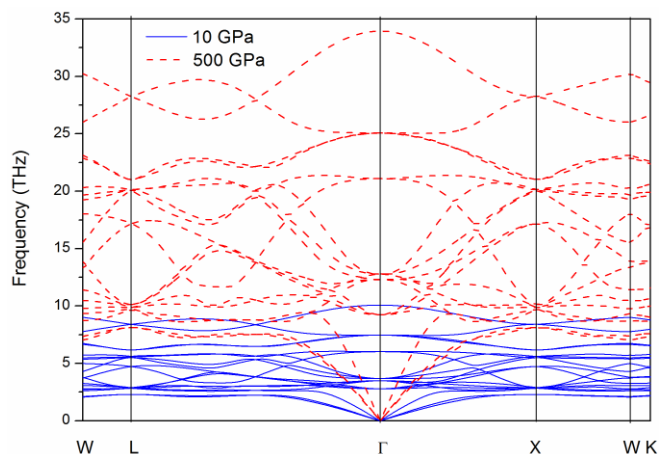


Figure 3. Phonon dispersion spectrum of XeAr_2 under different pressures.

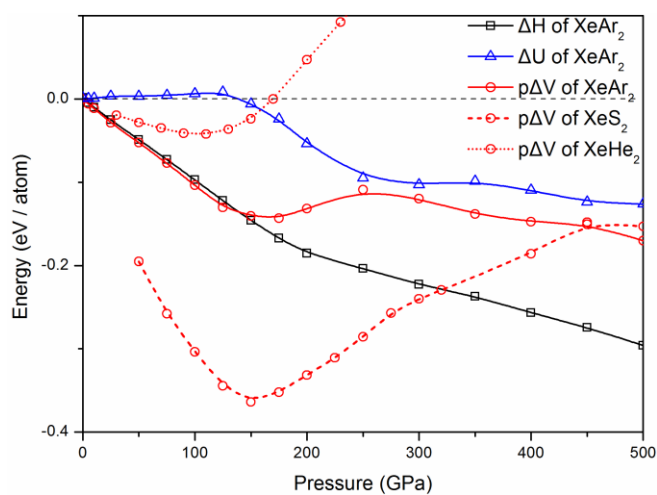


Figure 4. Pressure dependence of ΔH , ΔU , and $p\Delta V$ of relevant compounds.

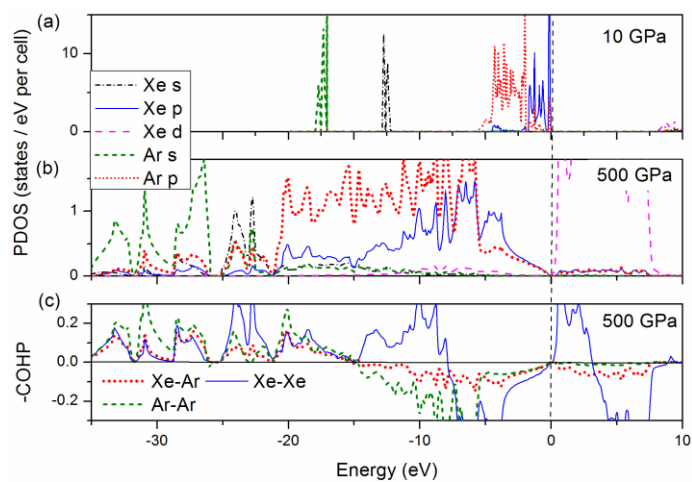


Figure 5. (a, b) Projected density of states (PDOS) of XeAr_2 at different pressures. (c) Crystal orbital Hamilton population (COHP) plots for nearest-neighboring Xe-Ar, Xe-Xe and Ar-Ar pairs at 500 GPa.